Inorganic Chemistry

ARTICLE

pubs.acs.org/IC

Ultrafast Spectroscopy of a Photochromic Ruthenium Sulfoxide Complex

Beth Anne McClure† and Jeffrey J. Rack*

Department of Chemistry and Biochemistry, Nanoscale and Quantum Phenomena Institute, Ohio University, Athens, Ohio 45701, United States

S *Supporting Information*

ABSTRACT: Photochromic $[Ru(bpy)_2(OSO)](PF_6)$, where bpy is 2,2′-bipyridine and OSO is 2-methylsulfinylbenzoate, was investigated by femtosecond transient absorption spectroscopy. The results show that for both S- and O-bonded isomers, a ^{3}MLCT state is formed on a femtosecond time scale. Also observed is the formation of multiple metal-to-ligand charge-transfer (MLCT) states, representing different conformers, prior to isomerization on the picosecond time scale. These results and others are compiled in an energy diagram depicting these results.

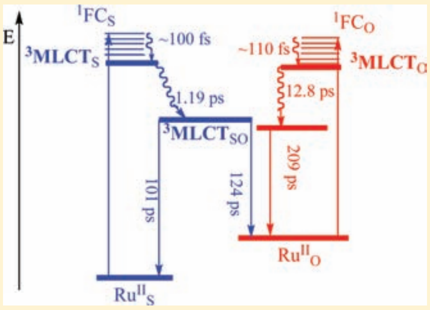

■ INTRODUCTION

Ultrafast visible spectroscopy reveals critical temporal information regarding the dynamics of electronic excited states of organic and inorganic dyes. These investigations have been particularly valuable for transition metal complexes related to $[Ru(bpy)_3]^{2+}$, where bpy is 2,2′-bipyridine.[1−7] A number of studies have shown that the vibrationally relaxed ^{3}MLCT excited state is formed on the femtosecond time scale even for low-symmetry derivatives.[8−11] From these and other related investigations, new approaches have emerged that aim to control excited state electron transfer through conformational changes of ligand structure on an ultrafast time scale, indicating the importance of these studies.[12−15]

For photochromic compounds, ultrafast spectroscopy reveals not only excited state dynamics but also information regarding excited state bond rupture and bond construction.[16] Such studies are critical for our understanding of these materials since a large nuclear reorganization immediately follows formation of the Franck−Condon states. These processes are concomitant with vibrational cooling, energy redistribution, and intersystem crossing and highlight the complexity of excited state dynamics in this group of chromophores.[17,18]

We have created a class of transition metal photochromes based on ruthenium polypyridine sulfoxide complexes, whose action is based on phototriggered S→O and O→S isomerization.[19−21] The large quantum yields of isomerization ($\Phi_{S\rightarrow O}$) indicate that these complexes efficiently convert photonic energy to potential energy for excited state bond breaking and forming reactions. Our previous reports on $[Ru(bpy)_2(OSO)]^+$, where OSO is 2-methylsulfinylbenzoate (Scheme 1), include the photochromic behavior ($\Phi_{S\rightarrow O} = 0.45$), isomerization kinetics, and spectral properties of both S- and O-bonded isomers (absorption spectra, Figure 1).[22−24] Herein, we report our first investigation on the femtosecond time scale, which reveals the formation of multiple ^{3}MLCT states prior to picosecond isomerization. We conclude with a complete energy diagram that depicts the reactivity of this complex.

■ RESULTS AND DISCUSSION

Shown in Figure 2 are the femtosecond transient absorption data for S-bonded $[Ru(bpy)_2(OSO)]^+$ in methanol solution. These spectral traces show the appearance of a bleach centered near 400 nm, an absorption peak at 360 nm, and a broad absorption from ~485 nm to longer wavelengths. In accordance with literature reports,[3,25] these features are ascribed to the loss of Ru^{II} MLCT absorption following excitation, to a $\pi^* \rightarrow \pi^*$ transition for the reduced bipyridine and to a bpy $\pi \rightarrow Ru^{III}$ LMCT transition, respectively. Global analysis of these data reveal a time constant of ~100 fs. The spectrum at 600 fs is representative of a relaxed metal-to-ligand charge-transfer (MLCT) excited state and is reminiscent of that observed at 300 fs in the ultrafast transient absorption spectroscopy of $[Ru(bpy)_3]^{2+}$.[2,3] Thus we interpret these data as corresponding to complete formation of the thermally equilibrated ^{3}MLCT state.

At longer time scales (Figure 3), the S-bonded ^{3}MLCT spectrum ultimately evolves to a spectrum at 502 ps that is identical to that of ground state O-bonded $[Ru(bpy)_2(OSO)]^+$ (see Figure 1 for comparison). This spectrum represents the ground state difference spectrum of O-bonded−S-bonded $[Ru(bpy)_2(OSO)]^+$. These data indicate that O-bonded $[Ru(bpy)_2(OSO)]^+$ produced from excitation of S-bonded

Received: March 15, 2011
Published: July 19, 2011

© 2011 American Chemical Society

Scheme 1. Isomers, Absorption Maxima and Reduction Potentials for Photochromic $[Ru(bpy)_2(OSO)]^+$

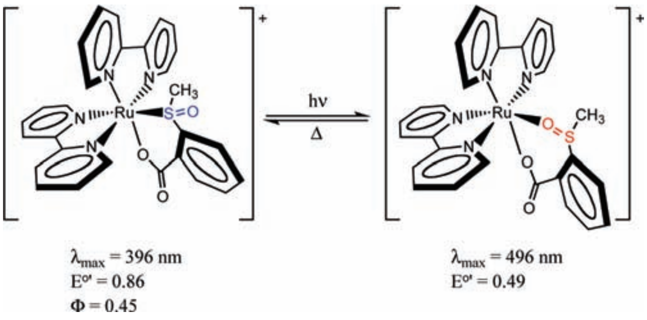

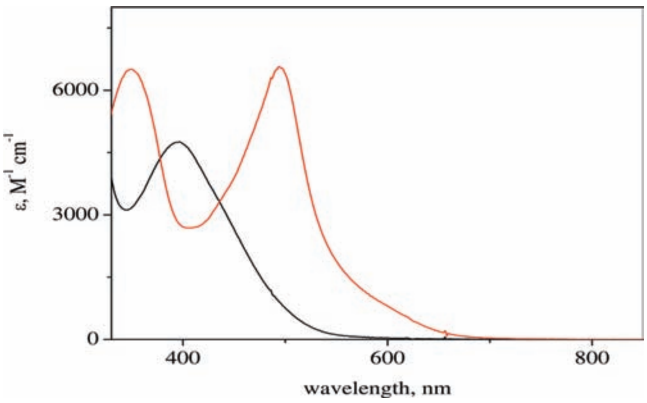

Figure 1. Absorption spectra of S-bonded (black) and O-bonded (red) $[Ru(bpy)_2(OSO)]^+$ in methanol solution.

$[Ru(bpy)_2(OSO)]^+$ is completely formed by 502 ps. The observation of an isosbestic point, the loss of the absorption at $\lambda > 600$ nm, and the appearance of an absorption at 500 nm, corresponding to ground state O-bonded $[Ru(bpy)_2(OSO)]^+$ support this assignment. In accord with global analysis results, single wavelength kinetic traces at 500 and 421 nm show the relaxation of these features to be bi-exponential yielding time constants of 1.01(±0.06) ps and 64.7(±2.3) ps at 500 nm, and 1.15(±0.20) ps and 55.5(±4.0) ps at 421 nm (Supporting Information, Figure S1). However, single wavelength kinetics at 361 nm also reveals a bi-exponential fit producing time constants of 0.84 (±0.17) ps, and $\tau_2 = 3.8$ (±1.8) ps (Supporting Information, Figure S2). The 0.84 ps time constant (361 nm) is within error of the 1.01 ps (500 nm) and 1.15 ps (421 nm) time constants and is interpreted as the transition from a ^{3}MLCT state of S-bonded character to the isomerizing state.[24] We tentatively ascribe the 3.8 ps kinetic phase at 361 nm to unspecified solvent motion. The absorption feature at this wavelength is due to the reduced bpy ligand and, at least in the case of $[Ru(bpy)_3]^{2+}$, is sensitive to solvent relaxation.[6] However, picosecond time-resolved resonance Raman,[4] time-resolved infrared,[26] and femtosecond visible transition absorption[3] spectroscopic data show vibrational relaxation on this time scale, suggesting that such processes may also contribute to the 3.8 ps kinetic phase at 361 nm.

In agreement with our previous results, we assign the 64.7 ps (500 nm) and 55.5 ps (421 nm) time constants as the conversion from a vibrationally relaxed ^{3}MLCT isomerizing state to both the S-bonded and O-bonded ground states. If isomerization ($k_{S\rightarrow O}$) and relaxation (k_R) to ground state occurs from this ^{3}MLCT state, then the quantum yield of isomerization is simply the isomerization rate constant divided by this sum ($k_{S\rightarrow O} + k_R$). Accordingly, with a quantum yield of 0.45, this yields a time constant of isomerization of $\tau_{S\rightarrow O} = 124(\pm 16)$ ps and agrees reasonably well with previous results (150 ps).[24]

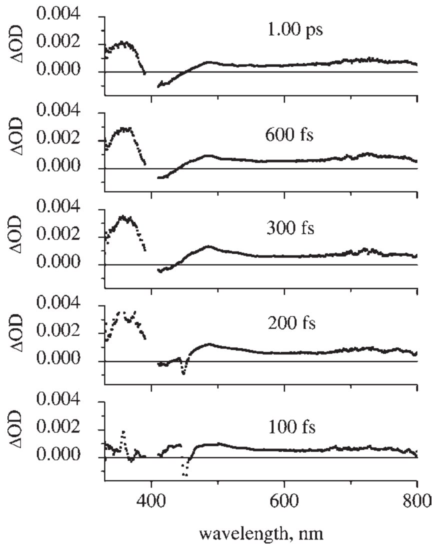

Figure 2. Stack plot of femtosecond transient absorption spectra of S-$[Ru(bpy)_2(OSO)]^+$ in methanol solution collected following 400 nm excitation. The missing data points around 400 nm are omitted for clarity. The sharp peaks at ~450 in the early time traces are due to unspecified Raman bands.

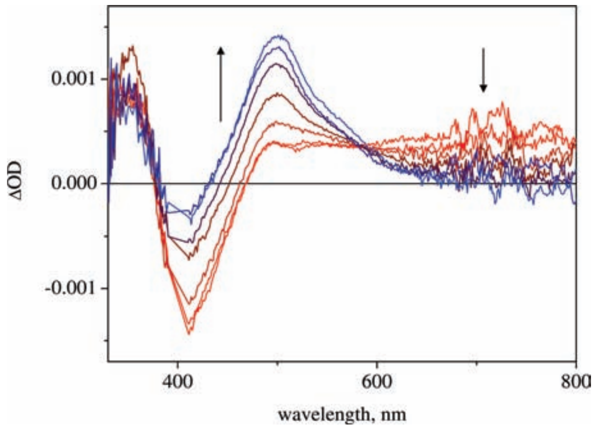

Figure 3. Transient absorption spectra of S-$[Ru(bpy)_2(OSO)]^+$ in methanol collected with 400 nm excitation. Spectral traces (from red to blue): 5.01 ps, 10.0 ps, 20.3 ps, 50.1 ps, 100 ps, 202 ps, 502 ps.

Shown in Figure 4 are the subpicosecond transient absorption data for O-bonded $[Ru(bpy)_2(OSO)]^+$ in methanol solution. Similar to the S-bonded isomer, the trace at 507 fs features an absorption at $\lambda > 600$ nm, a bleach near 500 nm, and an absorption at ~380 nm. Global analysis reveals a mono-exponential time constant of ~110 fs, similar to that observed for $[Ru(bpy)_3]^{2+}$. Thus, this time constant corresponds to the formation of the O-bonded ^{3}MLCT state from the initially prepared Franck–Condon states following excitation.

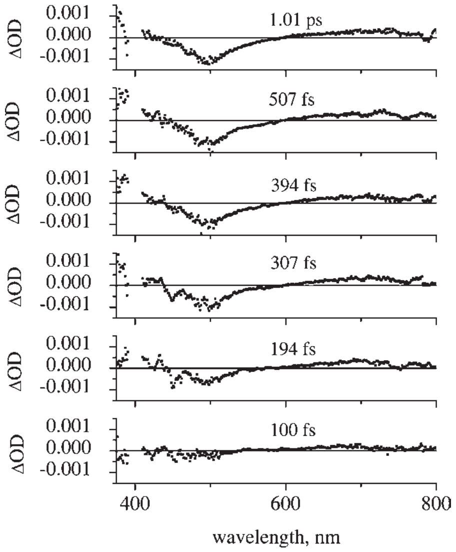

Figure 4. Stack plot of femtosecond transient absorption spectra of O-[Ru(bpy)$_2$(OSO)]$^+$ in methanol solution collected with 400 nm excitation. The missing data points around 400 nm are omitted for clarity.

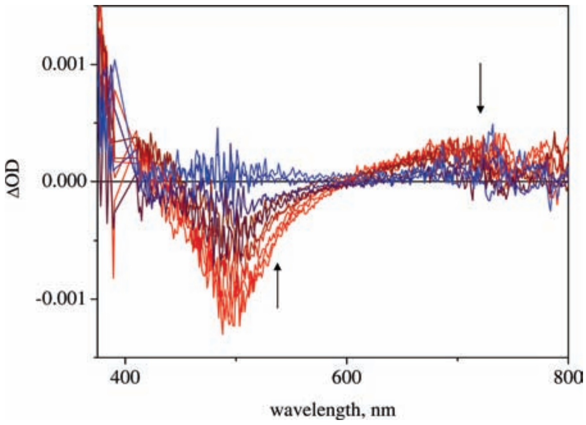

Figure 5. Transient absorption spectra of O-[Ru(bpy)$_2$(OSO)]$^+$ in methanol collected with 400 nm excitation. Spectral traces (red to blue): 1.01 ps, 2.01 ps, 5.00 ps, 10.1 ps, 20.5 ps, 50.0 ps, 102 ps, 202 ps, 503 ps, 883 ps.

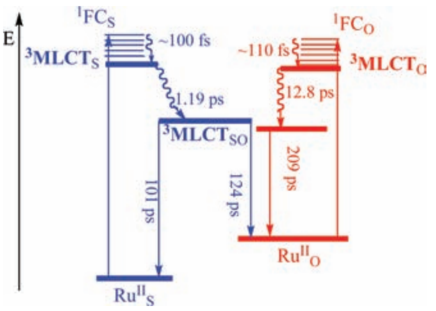

Figure 6. Energy Diagram of [Ru(bpy)$_2$(OSO)]$^+$ with kinetics.

Spectral traces collected at longer time delays show relaxation of the thermally equilibrated ^{3}MLCT state to form the O-bonded ground state, without evidence of additional products as indicated by a return to a zero baseline across the spectrum (Figure 5). This is consistent with our previous studies, which have found that the O-bonded isomer does not exhibit phototriggered reversible isomerization to the S-bonded isomer. However, a single wavelength kinetic trace at 500 nm reveals a bi-exponential decay with time constants of 12.8(±3.9) ps and 202(±70) ps (Supporting Information, Figure S3). Global analysis also exhibits bi-exponential behavior with similar kinetics. The spectral components (Supporting Information, Figure S4) for both time constants are quite similar and are consistent with an O-bonded ^{3}MLCT state. Importantly, the transient spectra do not show significant changes indicating that a species with different electronic features is not produced. If the shorter time constant were to correspond to a change in coordination sphere at the ruthenium as for the S-bonded isomer, a more significant difference in the spectral components might be expected. Given the time scale, we assign this event to a conformational change of the flexible benzoate moiety of the chelating sulfoxide ligand. This assignment is in accord with ground state time-resolved 2D-IR measurements performed on this compound, which show kinematic coupling between the symmetric and asymmetric carboxylate stretches and the sulfoxide stretch.[27,28] The long time constant is ascribed to formation of the O-bonded ground state.

An energy level diagram depicting the complete reactivity of [Ru(bpy)$_2$(OSO)]$^+$ is shown in Figure 6. Excitation of S-bonded [Ru(bpy)$_2$(OSO)]$^+$ yields Franck−Condon states (^{1}FC$_S$) on the ^{1}MLCT surface. These states rapidly relax to a vibrationally equilibrated S-bonded ^{3}MLCT with a time constant of ∼100 fs, consistent with many ultrafast literature reports on [Ru(bpy)$_3$]$^{2+}$. This state evolves to the isomerizing state, η^2-SO ^{3}MLCT. This kinetic component represents a partial isomerization of the sulfoxide ligand on the charge-transfer potential energy surface. We estimate η^2-SO ^{3}MLCT to be ∼1900 cm^{-1} lower than the S-bonded ^{3}MLCT ($E_S{}^{abs}$ = 25250 cm^{-1}; $E_S{}^{em}$ = 17240 cm^{-1}; ΔE = 8010 cm^{-1}).[23,24] We assume a 6000 cm^{-1} energy splitting from the initially formed Franck−Condon states to the thermally relaxed S-bonded ^{3}MLCT (includes contributions from singlet−triplet energy and reorganization energy) from [Ru(bpy)$_3$]$^{2+}$,[29,30] and that 77 K emission occurs from η^2-SO ^{3}MLCT. Nonadiabatic isomerization through a conical isomerization from the η^2-SO ^{3}MLCT to the singlet O-bonded surface ground state occurs on a longer time scale (124 ps).[24] The remainder of the isomerization occurs on the ground state potential energy surface. Similar to the S-bonded isomer, excitation of the O-bonded ground state produces Franck−Condon states (^{1}FC$_O$), which relax to an O-bonded ^{3}MLCT state. On the basis of absorption maxima ($E_S{}^{abs}$ = 25250 cm^{-1}; $E_O{}^{abs}$ = 20160 cm^{-1}) and ground state energies from electrochemical data ($E_S{}^{o\prime}$ = 0.86 V; $E_O{}^{o\prime}$ = 0.49 V vs Ag/AgPF$_6$ in propylene carbonate), ^{1}FC$_O$ is lower in energy than ^{1}FC$_S$. The initially formed O-bonded ^{3}MLCT state yields to another O-bonded ^{3}MLCT state (12.8 ps) that does not permit phototriggered reversion to the S-bonded state. As there is no evidence for photochemical conversion of the O-bonded isomer to the S-bonded isomer, we suspect that this state is lower in energy than η^2-SO ^{3}MLCT. The absence of any O-bonded emission (λ < 1000 nm) at 77 K complicates estimation of the relative energy of this state. Following formation of this new O-bonded ^{3}MLCT state, the ground state O-bonded isomer is produced with a time constant of 209 ps.

It is valuable to compare these results to other photoinduced isomerizations or rearrangements in other transition metal complexes.[31] Burkey and co-workers have investigated photoinduced ligand substitution reactions on organometallic tricarbonyl fragments by time-resolved infrared spectroscopy.[32,33] They showed that CO dissociation occurred on a picosecond time scale followed by ligand substitution within 200 ns, consistent with ligand rearrangement studies on $Cr(CO)_6$.[34] Investigations of hybrid platinum acetylene-dithienylethene complexes showed that charge-transfer excitation facilitated ring-closing of the dithienylethene photochrome through the acetylide bridge. While time-resolved data were not included in these reports, it is expected that this process occurs on the picosecond to nanoscale time scale.[35,36] Stilbene *trans*−*cis* isomerizations on $[Re(MeDpe)(CO)_3(bpy)]$, where MeDpe is a derivatized stilbene, have been investigated by Vlček by visible and infrared picosecond transient absorption spectroscopy.[37] These results show that MLCT (Re $d\pi \rightarrow$ bpy π^*) excitation induces trans→cis isomerization of the stilbene. Importantly, they assign a 21 ps kinetic component to partial isomerization of the stilbene along the ^{3}MLCT excited state surface. In conjunction with our data presented here, these reports demonstrate that large nuclear motions and ligand rearrangements on an electronic excited state occur on the picosecond time scale in transition metal complexes.

CONCLUSION

This femtosecond transient absorption study is the first report of the ultrafast dynamics of photochromic ruthenium sulfoxide complexes. The results clearly show the rapid formation ($\tau \sim 100$ fs) of a vibrationally equilibrated ^{3}MLCT state for both S- and O-bonded isomers, consistent with excited state evolution in $[Ru(bpy)_3]^{2+}$. Both isomers relax from these respective states to another lower energy ^{3}MLCT state. For the S-bonded isomer, this new state (η^2-SO) leads to isomerization, whereas for the O-bonded isomer, the newly formed state does not lead to isomerization. The appearance of new ^{3}MLCT states following the formation of vibrationally relaxed S- and O-bonded states indicates that large nuclear motions can occur on the ^{3}MLCT surface on a rapid time scale. Moreover, these observations suggest that there is strong mixing of vibrational and electronic wave functions (strong nonadiabatic coupling), consistent with the large $\Phi_{S\rightarrow O}$ and the rapid isomerization time constant (124 ps).

EXPERIMENTAL SECTION

The complex $[Ru(bpy)_2(OSO)](PF_6)$ was synthesized as described previously.[22,24] Methanol was purchased from VWR and used without further purification. Electronic absorption spectra were collected on an Agilent 8453 spectrophotometer. Femtosecond transient absorption measurements were collected on a Ultrafast Systems Helios transient absorption spectrometer (Ultrafast Systems). A Spectra Physics Solstice laser, a one-box regenerative amplifier which contains a Mai Tai femtosecond oscillator and Empower pump laser was used to produce 800 nm pulses at a repetition rate of 1 kHz at 3.5 W average power and a pulse width of <100 fs. From this unit, the beam is split (50:50) with one beam directed to an optical parametric amplifier (TOPAS, Light Conversion) and the other to the Helios spectrometer (HE-vis-3200) to create the pump (TOPAS) and probe (Helios) sources, respectively. The 400 nm pump beam was generated by fourth harmonic generation of the signal pulse. The 800 nm probe beam passed through a CaF_2 plate to generate a white light continuum (~330−850 nm). The spectrum was integrated for 2 s for each measurement, and results were averaged over 2 scans. A bulk sample solution of ~60 mL was prepared of the S-bonded isomer in methanol, which was flowed through a 2 mm path length cuvette to provide a fresh portion of solution for each spectrum collected. The O-bonded isomer was generated by irradiation of the S-bonded solution in a 2 mm path length cuvette with a 355 nm Nd:YAG 10 Hz pulse laser. Since there is no photochemical pathway for the O→S isomerization and the ground state O→S isomerization is slow ($t_{1/2} \sim 50$ h), irradiation produces a solution that is 100% O-isomer. The solution was stirred in the 2 mm path length cuvette during data collection. Transient absorption data were corrected by subtracting spectral background features that persisted from the previous pulse and appeared prepulse as well as applying chirp correction using Surface Xplorer Pro 1.1.5 software (Ultrafast Systems). The kinetics were fit using the global analysis function in Surface Xplorer Pro 1.1.5 software.

ASSOCIATED CONTENT

Supporting Information. Kinetic traces from transient absorption spectra, and O-bonded spectral components from global fit analysis. This material is available free of charge via the Internet at http://pubs.acs.org.

AUTHOR INFORMATION

Corresponding Author

*E-mail: rackj@ohio.edu.

Present Addresses

†Physical Biosciences Division, Lawrence Berkeley National Laboratory, Berkeley, CA 94720.

ACKNOWLEDGMENT

We thank Hugh Richardson and Greg Van Patten for helpful discussions. We acknowledge the NSF for funding (CHE 0809699 and CHE 0947031). B.A.M. thanks NDSEG for a graduate fellowship.

REFERENCES

(1) Bhasikuttan, A. C.; Suzuki, M.; Nakashima, S.; Okada, T. *J. Am. Chem. Soc.* **2002**, *124*, 8398–8405.

(2) Damrauer, N. H.; Cerullo, G.; Yeh, A.; Boussie, T. R.; Shank, C. V.; McCusker, J. K. *Science* **1997**, *275*, 54–57.

(3) Damrauer, N. H.; McCusker, J. K. *J. Phys. Chem. A* **1999**, *103*, 8440–8446.

(4) Henry, W.; Coates, C. G.; Brady, C.; Ronayne, K. L.; Matousek, P.; Towrie, M.; Botchway, S. W.; Parker, A. W.; Vos, J. G.; Browne, W. R.; McGarvey, J. J. *J. Phys. Chem. A* **2008**, *112*, 4537–4544.

(5) Yoon, S.; Kukura, P.; Stuart, C. M.; Mathies, R. A. *Mol. Phys.* **2006**, *104*, 1275–1282.

(6) Wallin, S.; Davidsson, J.; Modin, J.; Hammarstrom, L. *J. Phys. Chem. A* **2005**, *109*, 4697–4704.

(7) Yeh, A.; Shank, C. V.; McCusker, J. K. *Science* **2000**, *289*, 935–938.

(8) Henrich, J. D.; Zhang, H.; Dutta, P. K.; Kohler, B. *J. Phys. Chem. B* **2010**, *114*, 14679–14688.

(9) Liu, Y.; Turner, D. B.; Singh, T. N.; Angeles-Boza, A. M.; Chouai, A.; Dunbar, K. R.; Turro, C. *J. Am. Chem. Soc.* **2009**, *131*, 26–27.

(10) Sun, Y.; Liu, Y.; Turro, C. *J. Am. Chem. Soc.* **2010**, *132*, 5594–5595.

(11) Ramakrishna, G.; Jose, D. A.; Kumar, D. K.; Das, A.; Palit, D. K.; Ghosh, H. N. *J. Phys. Chem. B* **2006**, *110*, 10197–10203.

(12) Meylemans, H. A.; Hewitt, J. T.; Abdelhaq, M.; Vallett, P. J.; Damrauer, N. H. *J. Am. Chem. Soc.* **2010**, *132*, 11464–11466.

(13) Laine', P. P.; Campagna, S.; Loiseau, F. *Coord. Chem. Rev.* **2008**, *252*, 2552–2571.

(14) Rubtsov, I. V.; Redmore, N. P.; Hochstrasser, R. M.; Therien, M. J. *J. Am. Chem. Soc.* **2004**, *126*, 2684–2685.

(15) Meylemans, H. A.; Damrauer, N. H. *Inorg. Chem.* **2009**, *48*, 11161–11175.

(16) Tamai, N.; Miyasaka, H. *Chem. Rev.* **2000**, *100*, 1875–1890.

(17) Aloise, S.; Sliwa, M.; Pawlowska, Z.; Rehault, R.; Dubois, J.; Poizat, O.; Buntinx, G.; Perrier, A.; Maurel, F.; Yamaguchi, S.; Takeshita, M. *J. Am. Chem. Soc.* **2010**, *132*, 7379–7390.

(18) Buback, J.; Kullman, M.; Langhojer, F.; Nuernberger, P.; Schmidt, R.; Wurthner, F.; Brixner, T. *J. Am. Chem. Soc.* **2010**, *132*, 16510–16519.

(19) McClure, B. A.; Rack, J. J. *Eur. J. Inorg. Chem.* **2010**, 3895–3904.

(20) Rack, J. J. *Z. Kristallogr.* **2008**, *223*, 356–362.

(21) Rack, J. J. *Coord. Chem. Rev.* **2009**, *253*, 78–85.

(22) Butcher, D. P.; Rachford, A. A.; Petersen, J. L.; Rack, J. J. *Inorg. Chem.* **2006**, *45*, 9178–9180.

(23) McClure, B. A.; Abrams, E. R.; Rack, J. J. *J. Am. Chem. Soc.* **2010**, *132*, 5428–5436.

(24) McClure, B. A.; Mockus, N. V.; Butcher, D. P.; Lutterman, D. A.; Turro, C.; Petersen, J. L.; Rack, J. J. *Inorg. Chem.* **2009**, *48*, 8084–8091.

(25) Braterman, P. S.; Song, J.-I.; Peacock, R. D. *Inorg. Chem.* **1992**, *31*, 555–559.

(26) Liard, D. J.; Busby, M.; Matousek, P.; Towrie, M.; Vlček, A., Jr. *J. Phys. Chem. A* **2004**, *108*, 2363–2369.

(27) Keating, C. S.; McClure, B. A.; Rack, J. J.; Rubtsov, I. V. *J. Chem. Phys.* **2010**, *133*, 144513.

(28) Keating, C. S.; McClure, B. A.; Rack, J. J.; Rubtsov, I. V. *J. Phys. Chem. C* **2010**, *114*, 16740–16745.

(29) Daul, C.; Baerends, E. J.; Vernooijs, P. *Inorg. Chem.* **1994**, *33*, 3538–3543.

(30) Kober, E. M.; Meyer, T. J. *Inorg. Chem.* **1982**, *21*, 3967–3977.

(31) Vos, J. G.; Pryce, M. T. *Coord. Chem. Rev.* **2010**, *254*, 2519–2532.

(32) To, T. T.; Duke, C. B.; Junker, C. S.; O'Brien, C. M.; Ross, C. R.; Barnes, C. E.; Webster, C. E.; Burkey, T. J. *Organometallics* **2008**, *27*, 289–296.

(33) To, T. T.; Heilweil, E. J.; Duke, C. B.; Ruddick, K. R.; Webster, C. E.; Burkey, T. J. *J. Phys. Chem. A.* **2009**, *113*, 2666–2676.

(34) Shanoski, J. E.; Glascoe, E. A.; Harris, C. B. *J. Phys. Chem. B* **2006**, *110*, 996–1005.

(35) Roberts, M. N.; Carling, C. J.; Nagle, J. K.; Branda, N. R.; Wolf, M. O. *J. Am. Chem. Soc.* **2009**, *131*, 16644–5.

(36) Roberts, M. N.; Nagle, J. K.; Finden, J. G.; Branda, N. R.; Wolf, M. O. *Inorg. Chem.* **2009**, *48*, 19–21.

(37) Busby, M.; Hartl, F.; Matousek, P.; Towrie, M.; Vlček, A., Jr. *Chem.—Eur. J.* **2008**, *14*, 6912–6923.